
This is an electronic reprint of the original article.
This reprint may differ from the original in pagination and typographic detail.

Leino, Mikko; Islam, Mazidul; Ala-Laurinaho, Juha; Viikari, Ville
Diagnostics of the Phased Array for E-Band Using Holography Data

Published in:
Proceedings of the 48th European Microwave Conference

DOI:
[10.23919/EuMC.2018.8541725](https://doi.org/10.23919/EuMC.2018.8541725)

Published: 01/01/2018

Document Version
Peer-reviewed accepted author manuscript, also known as Final accepted manuscript or Post-print

Please cite the original version:
Leino, M., Islam, M., Ala-Laurinaho, J., & Viikari, V. (2018). Diagnostics of the Phased Array for E-Band Using Holography Data. In *Proceedings of the 48th European Microwave Conference* (pp. 1457-1460). (European Radar Conference EuRAD). IEEE. <https://doi.org/10.23919/EuMC.2018.8541725>

This material is protected by copyright and other intellectual property rights, and duplication or sale of all or part of any of the repository collections is not permitted, except that material may be duplicated by you for your research use or educational purposes in electronic or print form. You must obtain permission for any other use. Electronic or print copies may not be offered, whether for sale or otherwise to anyone who is not an authorised user.

This is the accepted version of the original article published by IEEE.

© 2018 IEEE. Personal use of this material is permitted. Permission from IEEE must be obtained for all other uses, in any current or future media, including reprinting/republishing this material for advertising or promotional purposes, creating new collective works, for resale or redistribution to servers or lists, or reuse of any copyrighted component of this work in other works.

Diagnostics of the Phased Array for E-band Using Holography Data

Mikko K. Leino¹, Md. Mazidul Islam², Juha Ala-Laurinaho³, Ville Viikari⁴

Department of Electronics and Nanoengineering, Aalto University, Finland
{¹mikko.k.leino, ²mazidul.islam, ³juha.ala-laurinaho, ⁴ville.viikari}@aalto.fi

Abstract— This paper presents antenna diagnostics of a 4 by 4 phased antenna array for 71–86 GHz, which could be potentially used as a future 5G access point. The antenna elements have their own phase shifters each and are fed from the one-port feeding network, which results in a challenge in single element performance analysis. To overcome this, the antenna has been measured with a near-field scanner and the acquired data is processed to form the holography presentation of the antenna radiation at its very aperture. The hologram results are further handled to analyze the phase shifters of each element and the operation of the feeding network over the observed frequency range. The mean amplitude and phase for the each element are calculated and the results are verified by calculation of the far-field using the processed values and compared to the far-field measurement results. The results show good agreement and the phase shifters work as intended resulting in the antenna beam steering accordingly. However, the feeding network is quite frequency-sensitive and it leaves much improvement especially for the 75–82 GHz band.

Keywords— Antenna measurements, Holography, Phased arrays, Phase shifters.

I. INTRODUCTION

Electrical beam steering in azimuth and elevation planes is a necessary requirement for the upcoming 5G base station antennas. One such antenna has been previously presented for E-band (71–86 GHz) in [1] and [2]. The presented antenna is a 4 by 4 phased array whose feeding network and antenna elements are waveguide-based to have low-losses. The feeding network is fed from one port and it consists of power dividers that divide the signal equally for each element. Between the feeding network and the antenna is a printed circuit board (PCB) where the signal phase is controlled. Each antenna element has a separate phase shifter implemented on the PCB.

The results presented in [1] suggest that the phased array gain is not as good as intended and a further evaluation of the each element is required. Initial near-field measurements of the feeding network alone indicate that the problem might be in its design and manufacturing, but further measurements are required to ensure that the transitions between the waveguides and the PCB are working. Furthermore, the phase shifters cannot be measured separately and thus their phase shifting capabilities have not been confirmed with the measurements. However, the one-port feed network makes the individual element analysis fairly challenging.

To overcome this problem, the antenna is measured using a near-field scanner, then the near-field data is processed and back-propagated to find the fields at the antenna aperture [3].

The resulting hologram presentation is utilized to characterize the individual element performance. For example, the defective elements in the array can be found this way as described in [4]. This paper presents how the measured near-field results can be handled and used for the evaluation of the each element and their corresponding phase shifters over the E-band.

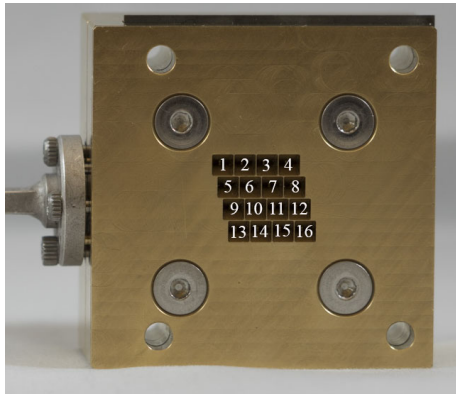
II. PHASED ARRAY

The antenna elements are pyramidal horn antennas that have a square aperture of the size of 3.1×3.1 mm². The array elements are slightly offset to avoid grating lobes in the radiation pattern. This means that the determination of the antenna element borders from the near-field data can be a bit more difficult than with the uniformly divided elements. The manufactured antenna structure is presented in Fig. 1a along with the element numbering. The feed network consists of the primary and the secondary power divider networks. The primary network divides the power equally from the single input to four similar waveguide outputs i.e. the antenna rows. This means that elements 1–4 are fed from one branch, elements 5–8 from the other etc. In these rows, the secondary networks are further used to subdivide the power equally to four elements, so that the total number of outputs and the elements is 16.

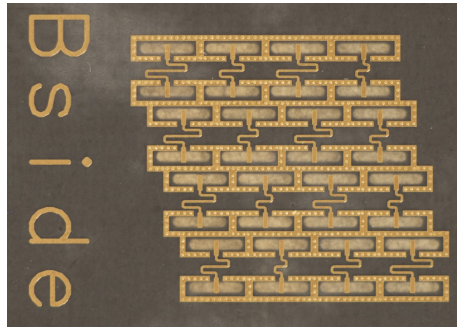
The beam of the characterized phased array is steered in azimuth, elevation, and diagonal directions. The required phase shift for each element has been calculated according to the wanted beam direction. The phase shifters to provide the required phase shifts are microstrip line-based true time delayed phase shifters, i.e. the electrical length and thus the phase delay will increase by increasing the physical length of the microstrip line.

Several PCBs have been manufactured with different microstrip line lengths to acquire the wanted phase shift for each element and to steer the beam to the wanted direction. Fig. 1b presents the PCB manufactured for the broadside-beam. In addition to the phase shifting capabilities of the phase shifters, their matching to the feed network is essential for the proper performance of the array. The PCB stack-up, the designed waveguide-to-PCB, and PCB-to-waveguide transitions are presented in more detail in [2].

Fourteen different PCBs that generate varying steering angles and beam directions have been measured as a part of the antenna. The frequency range for the measurements covers the E-band (71–86 GHz) with 0.5 GHz steps starting from the 71



(a)



(b)

Fig. 1. Manufactured parts: (a) antenna with WR-12 input, (b) phase shifters for broadside beam.

GHz. The antenna elements and phase shifters are evaluated for each frequency to find out common factors between different PCBs and possible frequency relations.

III. NEAR-FIELD MEASUREMENTS

The near-field measurements are done using a planar near-field scanner NSI-5x5 with open-ended waveguide WR12 (60–90 GHz) as a probe. The probe is aligned to the center of the antenna, the distance from the antenna is either 16 or 23 mm, and the near-field measurement resolution is 2 mm.

A reference horn antenna is measured over the observed bandwidth and used for the near-field data normalization. Thus the different PCB measurements at all the frequencies are comparable with each other, although the calibration of the VNA used in the measurements is not possible due to the measurement software. As the horn antenna has quite stable performance over the observed bandwidth, the normalization allows the different frequencies to be compared at the same amplitude range. This allows the comparable evaluations whether the elements are working or not as a function of the frequency.

IV. PHASED ARRAY ANALYSIS

The near-field measurement results are back-propagated to find out the antenna radiation at its very aperture. In the back-propagation, the near-field results are Fourier transformed to the angular frequency domain. Then the probe-corrected

electromagnetic fields are propagated towards the antenna, and finally the fields are inverse Fourier transformed back to the spatial domain to analyze the results. By increasing the Fourier transformation resolution and interpolating the fields between the measured points, we can increase the overall resolution that is suitable for further analysis. The fields at the array aperture plane for the measured antenna are calculated using the measurement software NSI-2000.

A. Hologram Analysis

The back-propagated fields in the aperture plane are called holograms, and they are visually evaluated with two-dimensional contour graphs to identify each antenna element in the array. This evaluation is critical as the center of the near-field measurement is not exactly aligned with the center of the antenna array. This is because antenna and the probe are aligned visually, causing the offset of millimeter decimals. One element has a square aperture of $3.1 \times 3.1 \text{ mm}^2$, so the offset must be carefully evaluated to acquire correct data from each element. Fig. 2 shows the normalized hologram for broadside at different frequencies.

After each element has been properly localized and identified, the phase and amplitude of the every element are evaluated separately. The mean amplitude and phase are calculated by taking the weighted average of the complex data points inside the element aperture. The weighting is done by applying a two-dimensional Tukey window (tapered cosine window) to the data so that the data points in the center of the element have higher weight than the ones near the element borders. This is done to reduce the effect of the adjacent elements in the analysis. For example, the amplitude data near the element borders is affected by the mutual coupling between

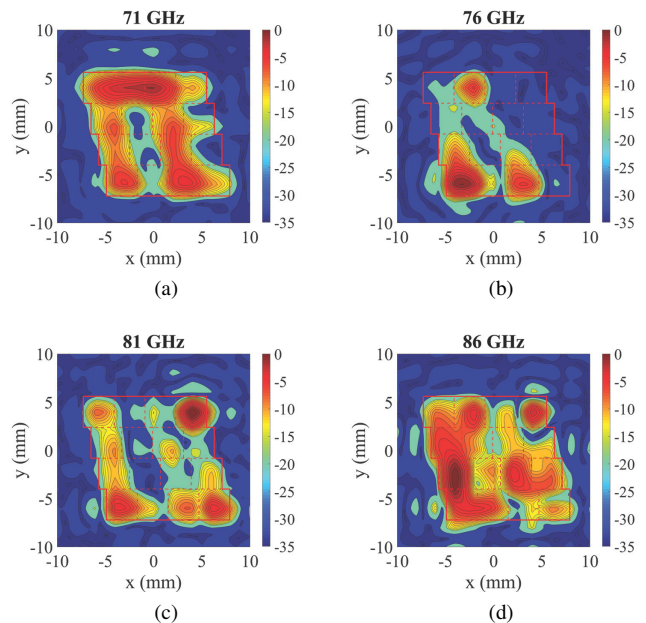


Fig. 2. Normalized hologram data for the broadside beam at (a) 71 GHz, (b) 76 GHz, (c) 81 GHz, and (d) 86 GHz.

the elements. Thus, the data near the edges can have higher amplitude values than a single element should have. Because we are interested in individual element performance, the effect of the mutual coupling is wanted to be low. Furthermore, the weighting is required, as there can still be some uncertainty of the actual position of the element in the hologram data. Thus, the data at the element borders is weighted to be zero.

After the normalization to the reference antenna mean amplitude, the mean amplitudes of each element are compared to the threshold level of -10 dB to evaluate whether the element is working. This is crucial as the feed network does not perform as intended over the whole frequency band, leaving some elements without power owing to the manufacturing and design flaws.

B. Individual Element Analysis

The phased array is evaluated for each frequency to find out how many elements out of the fourteen boards are working for that frequency. Additionally, a similar evaluation is done for the each element to see on if there is some frequency dependency in the element performance.

The analysis shows that the lower and higher frequencies of the observed frequency range have more working elements than the center frequencies. This can be seen well in Fig. 3. The lower band consists the frequencies between 71–74.5 GHz and the higher band the frequencies between 82.5–86 GHz. Although the performance and the working rate of the elements is limited at these frequencies, there is a clear difference in the performance compared to the center frequencies 75–82 GHz. It is also noticeable at the center frequencies that the last element of each branch is working particularly well, i.e. the elements 4, 8, 12, and 16 as seen in Fig. 3c. This indicates that the matching for the other elements is quite poor at those frequencies and that the primary power divider works as intended but the secondary network not, as most of the power flows through the last element in each branch.

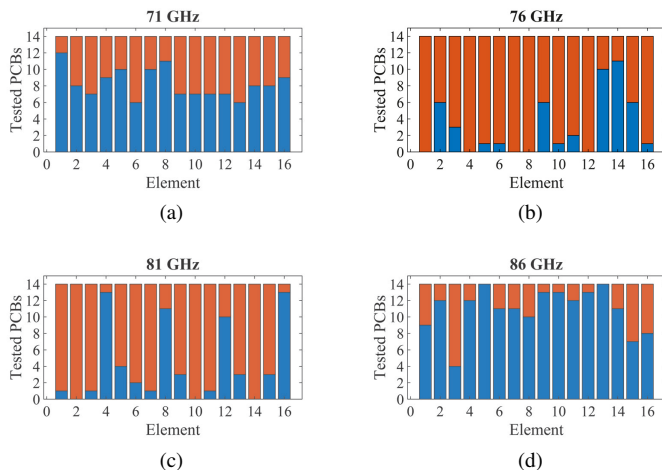


Fig. 3. Bar diagram shows how many elements of the tested PCBs are working (blue) and not (red) at (a) 71 GHz, (b) 76 GHz, (c) 81 GHz, and (d) 86 GHz.

By analyzing each element separately, the previous conclusion can be quite clearly seen. What is peculiar, however, is how the element performance can change quite drastically with the frequency. For example, the element 1 works well in most of the boards for the 71 and 71.5 GHz frequencies, but after that the performance drops drastically until it recovers as abruptly around the 84 GHz frequency as seen in Fig. 4. We can also notice the similar frequency dependence between the elements that are located at the same position in each column i.e. they are at the same point in the secondary power divider.

This phenomenon can be explained by the unwanted performance of the feed network. The first power divider seems to work fairly well regarding the operation frequency as each branch has somewhat similar amount of elements working when compared to each other. The problem could be that the secondary power divider is fairly frequency sensitive, especially when considering the matching to each element. The errors in the manufacturing and design are probable causes for internal reflections that can add destructively so that the signal is not coupled to all elements. Furthermore, the matching for each element might have deviated from the designed values resulting in the nonoptimal performance of the secondary power divider.

C. Validation of the Hologram Analysis

The weighted mean phases of each element are calculated similarly to the mean amplitude calculations by windowing the data for each element. Thus the hologram presentations of a weighted mean amplitude and phase are known for each element. This processed data is used to derive the far-field presentation of the antenna. The far-field is calculated considering the effect of the array factor but the element pattern is omitted from these calculations resulting in higher grating lobes. The acquired array factor results are then compared to the far-field results from the near-field measurements to validate whether the chosen data processing methods are suitable.

The results shown in Fig. 5 prove that the beam steers to the wanted directions with the designed PCBs and that the processed and unprocessed data result in similar far-field presentations. These results verify that the used data windowing is fairly well chosen and the elements who are working have a correct phase shift and the delayed line phase shifters, as well as the transitions between the waveguides and the PCB are working as intended. However, there is no power propagating through quite many elements. Thus, the antenna gain drops significantly, which is also seen in the measurement results.

V. CONCLUSION

The method of evaluating single elements of the phased array using the holography data from near-field measurements has been presented and validated as a suitable method for making antenna diagnostics evaluation. Through this evaluation, the performance of each element has been

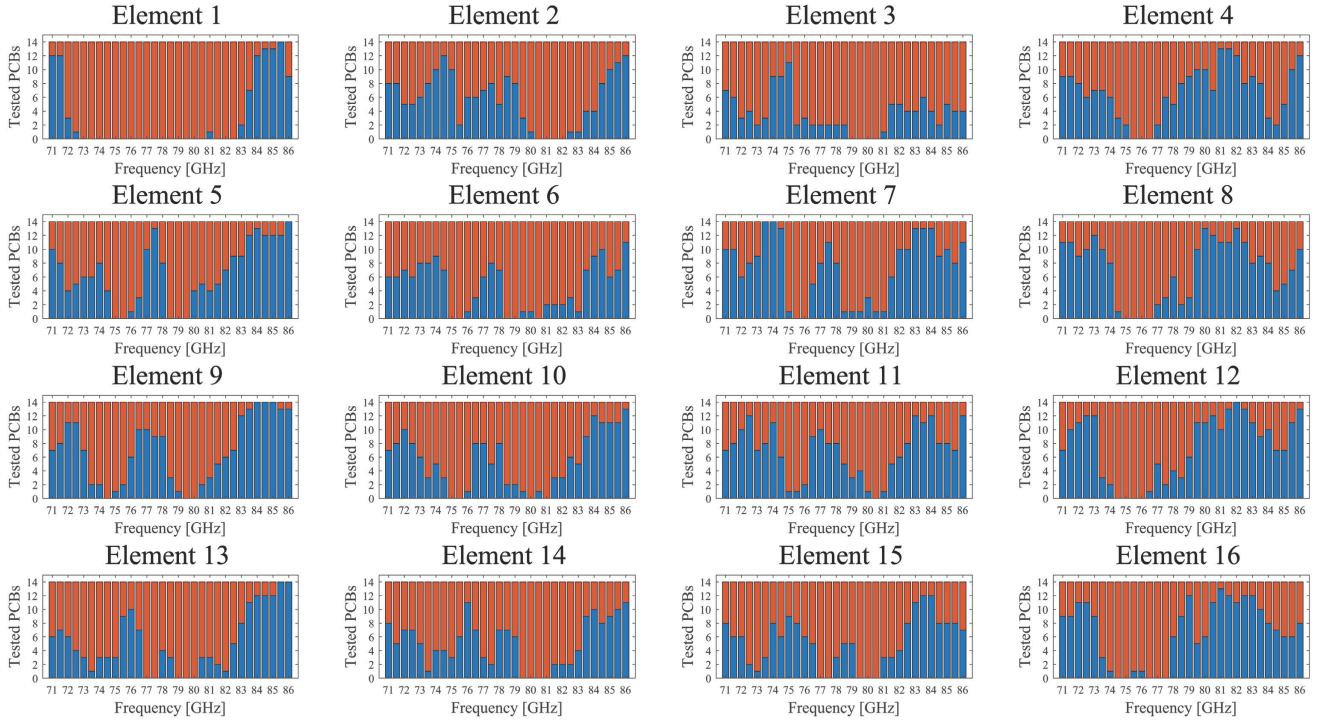


Fig. 4. Bar diagrams showing in how many tested PCBs the corresponding antenna element is working (blue) and not (red). These results are shown over the whole frequency range 71–86 GHz for each element.

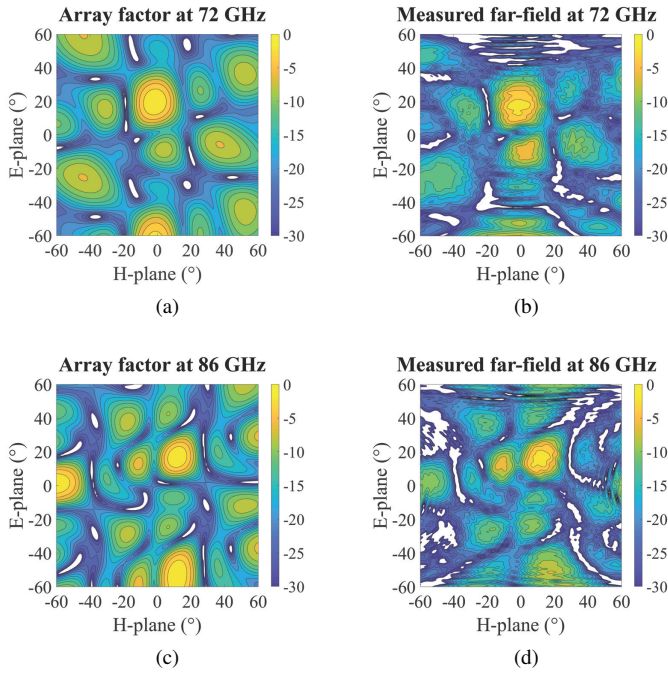


Fig. 5. Comparison of the 20° steered beams at far-field: (a) array factor at 72 GHz, (b) measured far-field at 72 GHz, (c) array factor at 86 GHz, and (d) measured far-field at 86 GHz.

diagnosed and the results prove that the designed phase shifters are working as intended. However, the power division network used to feed the antennas is not working over the whole E-band, but mainly at frequencies 71–74.5 GHz and 82.5–86

GHz. Especially the secondary power division network should be readjusted for the future designs as there is much to improve especially for the 75–82 GHz band.

ACKNOWLEDGMENT

Authors would like to thank Rasmus Luomaniemi for providing ideas for the measurements and how to present the acquired data.

REFERENCES

- [1] M. M. Islam, M. K. Leino, R. Luomaniemi, J. Song, R. Valkonen, J. Ala-Laurinaho, and V. Viikari, “E-band beam-steerable and scalable phase antenna array,” unpublished.
- [2] M. K. Leino, “Integrating phase shifters in a waveguide-fed antenna array,” Master’s thesis, Aalto University, Helsinki, Finland, 2017.
- [3] J. Hanfling, G. Borgiotti, and L. Kaplan, “The backward transform of the near field for reconstruction of aperture fields,” in *1979 Antennas and Propagation Society International Symposium*, vol. 17, June 1979, pp. 764–767.
- [4] J. J. Lee, E. M. Ferren, D. P. Woollen, and K. M. Lee, “Near-field probe used as a diagnostic tool to locate defective elements in an array antenna,” *IEEE Transactions on Antennas and Propagation*, vol. 36, no. 6, pp. 884–889, Jun 1988.